Spectroscopic analysis of Tm^{3+}:LuAG

2007 J. Phys.: Condens. Matter 19 036208

(http://iopscience.iop.org/0953-8984/19/3/036208)

INSTITUTE OF PHYSICS PUBLISHING JOURNAL OF PHYSICS: CONDENSED MATTER

J. Phys.: Condens. Matter **19** (2007) 036208 (10pp) doi:10.1088/0953-8984/19/3/036208

Spectroscopic analysis of Tm^{3+}:LuAG

Hamit Kalaycioglu[1], **Alphan Sennaroglu**[1,3], **Adnan Kurt**[1] **and Gonul Ozen**[2]

[1] Laser Research Laboratory, Department of Physics, Koç University Rumelifeneri Yolu, Sariyer 34450 Istanbul, Turkey
[2] Department of Physics, Istanbul Technical University Maslak, 34469 Istanbul, Turkey

E-mail: asennar@ku.edu.tr

Received 2 August 2006, in final form 18 November 2006
Published 5 January 2007
Online at stacks.iop.org/JPhysCM/19/036208

Abstract

We studied the spectroscopic properties of two thulium-doped $Lu_3Al_5O_{12}$ (Tm:LuAG) samples with Tm^{3+} concentrations of 0.5 and 5 at.%. Judd–Ofelt theory was used to analyse the absorption spectra and to determine the radiative transition rates. Fluorescence measurements were further performed to determine the luminescence quantum efficiencies. The average radiative lifetimes of the $^3H_4$ and $^3F_4$ levels were calculated to be 1041 ± 143 μs and 17.7 ± 3.4 ms, respectively. We observed a sharp increase in the strength of cross relaxation for the 5% Tm:LuAG sample evidenced by the much shorter fluorescence lifetime of 42.3 μs for the $^3H_4$ level, in comparison with 851 μs for the 0.5% Tm:LuAG sample. This was further supported by the relative emission measurements at 1470 and 1800 nm. The measured fluorescence lifetime of the $^3F_4$ level showed a smaller decrease from 11.2 ms (0.5% doping) to 7.1 ms (5% doping). By using the Judd–Ofelt theory, the stimulated emission cross section was further calculated to be $1.2 \pm 0.2 \times 10^{-21}$ cm^2 at 2023 nm, corresponding to the free running wavelength of Tm:LuAG lasers. Finally, the critical distance parameter R_0 for cross relaxation was determined to be 10.2 ± 0.8 Å from the fluorescence decay data.

(Some figures in this article are in colour only in the electronic version)

1. Introduction

Lasing experiments done with thulium-doped $Lu_3Al_5O_{12}$ (Tm:LuAG) crystals have demonstrated their potential as versatile sources of coherent radiation at 2 μm [1–4]. Also, Filer *et al* showed, based on a quantum mechanical model, that LuAG has the best figure of merit and the lowest lasing threshold for the 2 μm transition among several other thulium-doped

[3] Author to whom any correspondence should be addressed.

garnets [5]. In this work, the figure of merit (FOM) was defined as the ratio of the thulium ions in the $^3F_4$ level at the lasing threshold to the total number of thulium ions and comes to 0.06 for the 2.07 μm emission line of LuAG. For comparison, the calculated value of FOM is 0.08 for the YAG (2.04 μm emission) and YScAG (2.03 μm emission) hosts, indicating higher lasing thresholds [5]. In free-running mode, Tm:LuAG lasers operate at 2.023 μm, which is in one of the preferred wavelength ranges for lidar applications [4]. Similar to other thulium-based lasers, they can be directly diode-pumped by using pumps operating in the 780–790 nm range [1, 3, 4]. Based on these facts, we believe the spectroscopic characteristics of Tm:LuAG deserve a detailed investigation which, to the best of our knowledge, has not been undertaken.

In this paper, we present the results of spectroscopic measurements and analyses done on two Tm:LuAG crystals with Tm^{3+} ion concentrations of 0.5 and 5 at.% (hereafter referred to as 0.5% Tm:LuAG and 5% Tm:LuAG, respectively, in the text). In the experiments, absorption and fluorescence spectra were recorded and intensity parameters (Ω_2, Ω_4, Ω_6), radiative lifetimes of the $^3H_4$ and $^3F_4$ levels and emission cross sections of the $^3F_4 \rightarrow {}^3H_6$ transition were calculated using the Judd–Ofelt theory (see figure 1 which shows the energy-level diagram for Tm:LuAG). Fluorescence lifetimes of the $^3H_4$ and $^3F_4$ levels were measured and luminescence quantum efficiencies for the $^3H_4 \rightarrow {}^3H_6$ (1470 nm band) and $^3F_4 \rightarrow {}^3H_6$ (1800 nm band) transitions were determined. Finally, the lifetime data were used to estimate the average critical distance parameter R_0 which gives a measure of the strength of cross relaxation [6]. Our measurements show that the lifetime of the $^3F_4$ level decreases from 11.2 ms for 0.5% Tm:LuAG to 7.1 ms for the 5% Tm:LuAG sample. The measured lifetime of the $^3H_4$ level drops sharply from 851 μs for the 0.5% doped sample to 42.3 μs for the 5% doped sample due to the effect of cross relaxation. The substantial decrease in the lifetime of the $^3H_4$ level is also implied by the vanishing fluorescence of the 1470 nm band in the highly doped sample. The luminescence quantum efficiency of the 1800 nm band was determined to be 0.63 ± 0.12 and 0.40 ± 0.08 for the 0.5% and 5% Tm:LuAG samples, respectively, whereas for the 1470 nm band it was determined to be 0.82 ± 0.11 and 0.04 ± 0.006 for the 0.5% and 5% Tm:LuAG samples, respectively. The emission cross section for the 2023 nm emission peak was calculated to be $1.2 \pm 0.2 \times 10^{-21}$ cm^2, and the critical distance parameter R_0 was determined to be 10.2 ± 0.8 Å, both representing the average of the two samples.

2. Experimental details

Two samples of Tm:LuAG with 0.5 and 5 at.% Tm^+ concentration were supplied by the Scientific Materials Corporation, USA. The density of the samples was measured with a pycnometer, using Archimedes' principle, to be 6.317 g cm^{-3}.

The absorption spectra of the samples were measured with a spectrophotometer in the 190–2500 nm range at room temperature. In the fluorescence measurements, the samples were excited by a continuous-wave diode laser emitting at 785 nm and the collected fluorescence signal was fed into a Czerny–Turner-type monochromator. After passing through the monochromator, the signal was detected with a PbS detector and sent to an electronic amplifying and digitizing circuit. The resulting spectra were corrected for the detector and diffraction grating response. To measure the lifetimes of the $^3H_4$ and $^3F_4$ levels, the crystals were excited with a pulsed Ti:sapphire laser whose operating wavelength was tuned to 788 nm to maximize the fluorescence intensity. The pulsewidth of the pump source was 70 ns. For the $^3H_4$ lifetime, the Ti^{3+}:sapphire was operated at 1 kHz, and the fluorescence decay at 823 nm corresponding to $^3H_4 \rightarrow {}^3H_6$ transition was filtered through a monochromator and recorded with the help of a photomultiplier tube sensitive up to 900 nm range. For the $^3F_4$ lifetime, the pump source was operated at 100 Hz, and fluorescence decay due to $^3F_4 \rightarrow {}^3H_6$ transition was

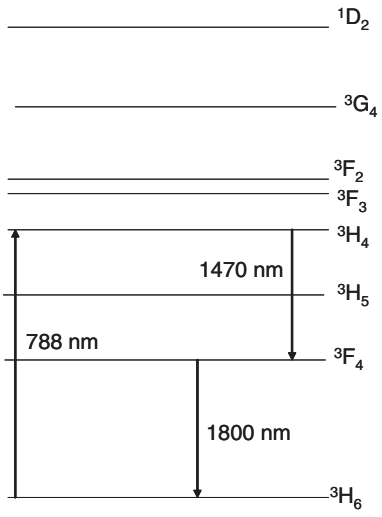

Figure 1. Energy-level diagram of Tm^{3+} ions in LuAG.

recorded with a germanium detector after the fluorescence from the $^3H_4$ level was eliminated by using long-pass filters.

3. Results and discussion

3.1. Judd–Ofelt analysis

Figures 2(a)–(d) show the absorption spectra (absorption coefficient versus wavelength) of the samples for the 190–990 nm and 1000–2000 nm ranges. The absorption bands corresponding to the ground-state ($^3H_6$) absorption of the $^1D_2$, $^1G_4$, $^3F_2$, $^3F_3$, $^3H_4$, $^3H_5$ and $^3F_4$ levels (see figure 1) are indicated in these graphs. It is observed that the peak absorption wavelength for the $^3H_6 \rightarrow {}^3H_4$ transition is 788 nm, and an average absorption cross section of 5.37×10^{-21} cm^2 is calculated at this wavelength.

In order to apply the reciprocity method based on the Judd–Ofelt theory [7, 8], the integrated absorption coefficient (spectral intensity) for each indicated absorption band was calculated by using

$$(\Sigma_\mu)_{\text{exp}} = \int_{\text{band}} \mu(\lambda)\, \mathrm{d}\lambda, \tag{1}$$

where $\mu(\lambda)$ is the measured absorption coefficient. Background correction was applied to each absorption band before integrating it.

In the previous work of Van Vleck [9] and Broer *et al* [10], it was shown that electric-dipole transitions are the dominant processes in crystals doped with lanthanide (Ln^{3+}) ions. In most cases, electric dipole transitions dictate the spectroscopic properties of Ln^{3+}-doped crystals [11]. On the other hand, magnetic dipole transitions which obey the selection rules $\Delta J \leqslant 1$, $\Delta L = 0$, $\Delta S = 0$ and $\Delta l = 0$, play a significant role in only a few transitions of Ln^{3+} ions. For the spectral range used in our analysis, magnetic dipole transitions can be neglected for the Tm^{3+} ion [12]. Judd–Ofelt theory [7, 8] states that the integrated absorption coefficient $(\Sigma_\mu)_{\text{calc}}$ of an electric-dipole transition from the ground state (SLJ) to the excited

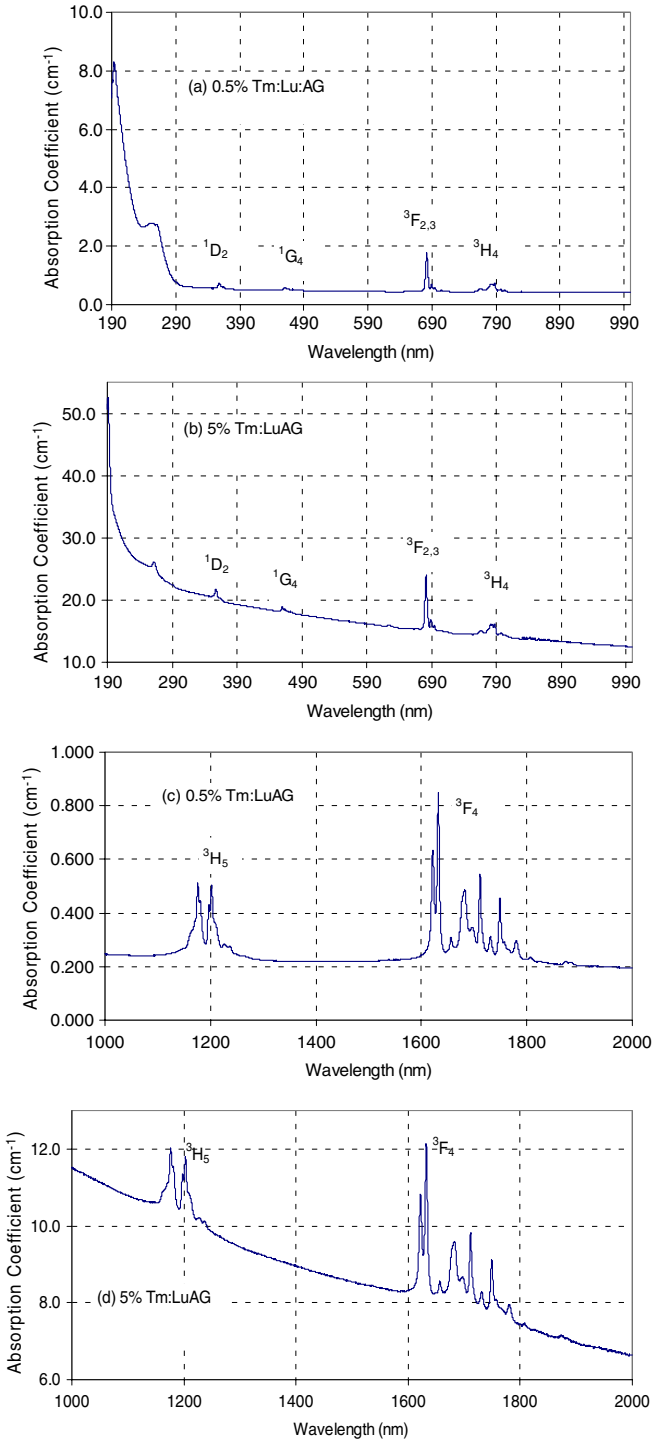

Figure 2. Absorption spectra of the Tm:LuAG samples with (a) 0.5% Tm^{3+} concentration in the range 190–990 nm, (b) 5% Tm^{3+} concentration in the range 190–990 nm, (c) 0.5% Tm^{3+} concentration in the range 1000–2000 nm and (d) 5% Tm^{3+} concentration in the range 1000–2000 nm.

Table 1. Measured and calculated integrated absorption coefficients and root-mean square error for the Tm:LuAG samples.

Transition from $^3H_6 \rightarrow$	0.5% Tm:LuAG		5% Tm:LuAG	
	$(\Sigma_\mu)_{exp}$ (10^{-6})	$(\Sigma_\mu)_{calc}$ (10^{-6})	$(\Sigma_\mu)_{exp}$ (10^{-6})	$(\Sigma_\mu)_{calc}$ (10^{-6})
$^1D_2$	0.15	0.11	0.96	0.66
$^1G_4$	0.09	0.04	0.57	0.30
$^3F_{23}$	0.86	0.84	5.48	5.22
$^3H_4$	0.58	0.55	4.25	3.98
$^3H_5$	0.91	0.94	5.76	6.20
$^3F_4$	1.58	1.58	12.2	12.2
σ_{rms} (10^{-7})	0.45		4.1	

state $(S'L'J')$ can be calculated from

$$(\Sigma_\mu)_{calc} = \frac{8\pi^3 e^2}{3ch}\frac{(n^2+2)^2}{9n}\frac{\bar{\lambda}}{(2J+1)}N_0 \sum_{t=2,4,6} \Omega_t \left|\left\langle SLJ \left\| U^{(t)} \right\| S'L'J' \right\rangle\right|^2, \tag{2}$$

where $\bar{\lambda}$ is the mean wavelength of the absorption band or bands for overlapping cases, n is the refractive index, c is the speed of light, h is Planck's constant, J is the total angular momentum quantum number of the ground state, N_0 is the Tm^{3+} concentration in the crystal, $U^{(t)}$ are the doubly reduced matrix elements of the unit tensor operator of rank t and Ω_t are the Judd–Ofelt intensity parameters. Ω_t values were approximately calculated by solving the over-determined system of six equations from six absorption bands with a matrix inversion method. Since the matrix elements $U^{(t)}$ are not strongly host dependent [13], values tabulated by Kamiskii [14] were used in this calculation. N_0 (6.7×10^{19} cm^{-3} for the 0.5% Tm:LuAG) was determined using the sample concentration and measured density. The root-mean square error

$$\sigma_{rms} = \sqrt{\frac{\sum (f_{cal} - f_{exp})^2}{q-p}} \tag{3}$$

indicates the proximity of the approximation. In equation (3), q represents the number of bands for which line strengths are calculated (six in our case) and p the number of parameters determined (three in our case). The resulting experimental and calculated line strengths (f_{exp} and f_{cal}), together with σ_{rms} for both samples, are listed in table 1.

Once the intensity parameters Ω_t are determined, the spontaneous emission probability (rate) $A(J, J')$ for an electric-dipole transition from a SLJ state to a $S'L'J'$ state with a mean wavenumber $\bar{\nu}$ can be calculated using

$$A(J, J') = \frac{64\pi^4 e^2}{3h(2J+1)}\frac{n(n^2+2)^2\bar{\nu}^3}{9} \sum_{t=2,4,6} \Omega_t \left|\left\langle SLJ \left\| U^{(t)} \right\| S'L'J' \right\rangle\right|^2. \tag{4}$$

The radiative lifetime τ_R of an excited state given by

$$\tau_R = \frac{1}{\sum_j A(i, j)} \tag{5}$$

equals the inverse of the total spontaneous emission probability from the excited state which is the sum of the transition rates to all possible lower states. Table 2 lists the intensity parameters Ω_t and the radiative lifetimes τ_R of the $^3F_4$ and $^3H_4$ states obtained from the Judd–Ofelt analysis. Since the intensity parameters are expected to be independent of the doping concentration, the average values of Ω_t shown in table 2 were used in the calculation

Table 2. Calculated values of the intensity parameters and the radiative lifetimes of the $^3F_4$ and $^3H_4$ levels for the Tm:LuAG samples.

Tm:LuAG sample	Ω_2 (10^{-21} cm^2)	Ω_4 (10^{-21} cm^2)	Ω_6 (10^{-21} cm^2)	τ_R (μs) $^3H_4$	τ_R (ms) $^3F_4$
0.5%	4.39	8.08	10.5	917.6	14.9
5%	5.93	4.84	6.59	1203.8	21.7
Average	$5.16 \pm 15\%$	$6.46 \pm 25\%$	$8.55 \pm 23\%$	1041.4 ± 143 [a]	17.7 ± 3.4 [a]

[a] Calculated by using the average intensity parameters from this table.

of τ_R. Also, we included in table 2 the estimated error in each parameter originating from the difference between the calculated intensity parameters for the two samples. The uncertainty in our results is comparable to the expected accuracy limit for the Judd–Ofelt model [15]. In calculating the lifetimes of the $^3F_4$ (1800 nm) and $^3H_4$ (1470 nm) levels, the tabulated matrix elements $|\langle SLJ\|U^{(t)}\|S'L'J'\rangle|^2$ in [14] were used.

3.2. Fluorescence spectroscopy and analysis

Figures 3(a) and (b) show the fluorescence spectra of the two Tm:LuAG samples for the 1000–2500 nm range. The disappearance of the 1470 nm ($^3H_4 \rightarrow {}^3F_4$) emission band for the sample with higher Tm^{3+} concentration (figure 3(b)) indicates strong cross relaxation. A similar effect was observed in other thulium-doped materials [16, 17]. Cross relaxation processes occur increasingly with the growing density of the Tm^{3+} ions inside the host crystal lattice and enhance the nonradiative decay of the $^3H_4$ level in favour of the 1800 nm ($^3F_4 \rightarrow {}^3H_6$) emission. This effect is exploited for the enhancement of the lasing efficiency in thulium lasers operating at 2 μm. During this process, a Tm^{3+} ion, excited to the $^3H_4$ level by the pump radiation, stimulates, as it decays nonradiatively to the $^3F_4$ level, a nearby ion to move from the ground ($^3H_6$) state to the $^3F_4$ state. The vanishing 1470 nm band points to the evident growth in the strength of cross relaxation as the Tm^{3+} concentration increases 10-fold and the proximity of ions increases.

The fluorescence spectra were used to calculate the stimulated emission cross section σ_{em} for the $^3F_4 \rightarrow {}^3H_6$ (1800 nm) transition using the Fuchtbauer–Ladenburg equation [18, 19]:

$$\sigma_{em}(\lambda) = \frac{\lambda^5 I(\lambda) A(J, J')}{8\pi n^2 c \int I(\lambda)\lambda \, d\lambda} \tag{6}$$

where $I(\lambda)$ is the normalized fluorescence intensity at wavelength λ. In this calculation, spontaneous emission rates $A(J, J')$ based on average intensity parameters were used. The calculated σ_{em}, for the two samples, at 1754, 1969 and 2023 nm peaks inside the 1800 nm band are presented in table 3. Among the three peaks, the highest σ_{em} value of $1.2 \pm 0.2 \times 10^{-21}$ cm^2 (average of the two samples) occurring at 2023 nm is in reasonable agreement with the value (1.66×10^{-21} cm^2) reported in [4]. It also agrees with the free-running wavelength of the Tm:LuAG laser.

The recorded fluorescence decay curves of the $^3F_4$ and $^3H_4$ levels for both samples are shown in figures 4 and 5, respectively. The initial rise in the decay curve of the $^3F_4$ level (see figure 4) is a result of the gradual build-up of this level, as the ions initially excited to the $^3H_4$ level by the pump radiation decay after a finite time to populate the $^3F_4$ level. The initial build-up effect is notably more visible in the 0.5% Tm:LuAG sample in which the decay of the $^3H_4$ level is significantly slower than that in the 5% Tm:LuAG sample. The faster decay of the $^3H_4$ level for the 5% sample is clearly observed in figure 5, where the timescale for the

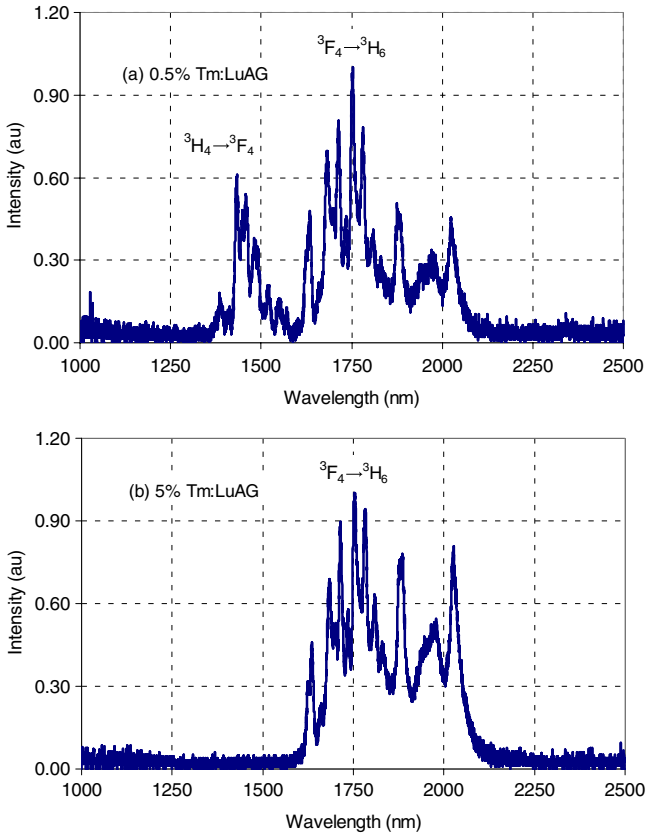

Figure 3. Fluorescence spectra of the (a) 0.5% Tm:LuAG and (b) 5% Tm:LuAG samples. Emission bands corresponding to the $^3H_4 \rightarrow {}^3F_4$ and $^3F_4 \rightarrow {}^3H_6$ transitions are indicated.

Table 3. Stimulated emission cross sections for three peaks of the $^3F_4 \rightarrow {}^3H_4$ (1800 nm) transition.

Tm:LuAG sample	σ_{se} (10^{-21} cm^2)		
	1754 nm	1969 nm	2023 nm
0.5%	1.36 ± 0.26	0.71 ± 0.13	1.11 ± 0.21
5%	0.93 ± 0.18	0.84 ± 0.16	1.38 ± 0.26
Average	1.15 ± 0.22	0.78 ± 0.15	1.24 ± 0.24

decay of this level is about 20 times larger for the 0.5% Tm:LuAG sample. As discussed above, the cross relaxation effect is mainly responsible for the sharp increase in the decay rate of the $^3H_4$ level with increasing concentration. The measured fluorescence lifetimes τ_F of the $^3H_4$ and $^3F_4$ levels were determined by fitting the tail of each fluorescence decay curve to a single exponential. Table 4 lists for both samples the measured lifetimes τ_F and the corresponding luminescence efficiencies η defined according to

$$\eta = \frac{\tau_F}{\tau_R}, \tag{7}$$

where τ_R is the radiative lifetime given in equation (5). In calculating the luminescence efficiency, average radiative lifetimes resulting from the Judd–Ofelt analysis (see table 2)

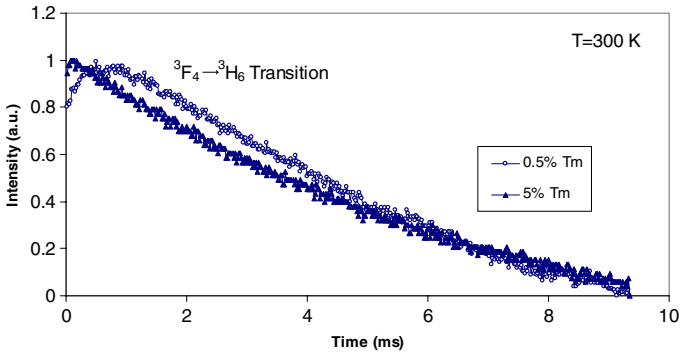

Figure 4. Measured fluorescence decay curves of the $^3F_4$ level for the two Tm:LuAG samples.

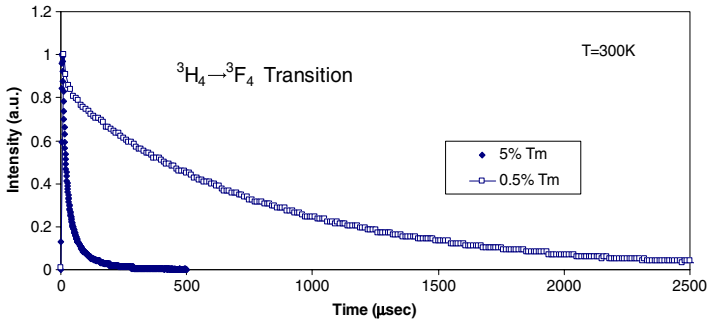

Figure 5. Measured fluorescence decay curves of the $^3H_4$ level for the two Tm:LuAG samples.

Table 4. Fluorescence lifetimes τ_F and fluorescence quantum efficiencies η for the Tm:LuAG samples.

Tm:LuAG sample	τ_F (μs) $^3H_4$	τ_F (ms) $^3F_4$	η $^3H_4$	η $^3F_4$
0.5%	851	11.2	0.82 ± 0.11	0.63 ± 0.12
5%	42.3	7.1	0.041 ± 0.006	0.40 ± 0.08

were used. The decrease from 11.2 ms for the 0.5% Tm:LuAG sample to 7.1 ms for the 5% Tm:LuAG sample in the lifetime of the $^3F_4$ level also indicates the effect of increasing nonradiative processes with denser population of Tm^{3+} ions inside the lattice. Comparable variations of lifetime with Tm^{3+} concentration have been reported for other host crystals and glasses [6, 16, 17]. The average lifetime value determined in our study is somewhat lower than the value of 10.2 ms reported in [3] for the $^3F_4$ lifetime of Tm:LuAG samples with Tm^{3+} concentration varying from 2 to 11%.

The mechanism of cross relaxation which involves energy transfer between Tm^{3+} ions was described as a diffusion-limited relaxation process, rather than the other possibilities of direct relaxation and fast diffusion [20]. In such a process, population of the excited level $N(t)$ is modelled by [6]

$$N(t) = \exp\left[-t/\tau_R - \Pi(t)\right] \tag{8}$$

where τ_R is the radiative lifetime and $\Pi(t)$ accounts for the deviation from a single exponential decay that would occur if the excited ions were to decay intrinsically in the absence of acceptors

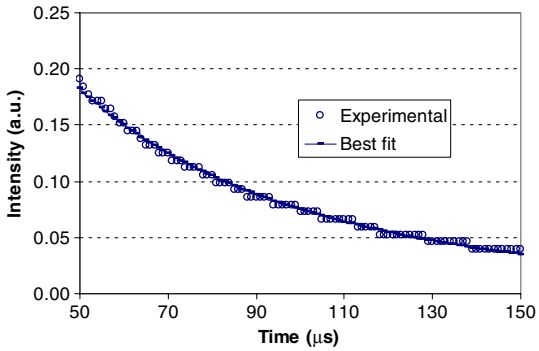

Figure 6. Measured fluorescence decay of the $^3F_4 \rightarrow {}^3H_4$ transition and calculated best fit to equations (8) and (9) for the 5% Tm:LuAG sample.

and energy diffusion [20]. In a diffusion-limited relaxation process, Yokota and Tanimoto [21] showed that the deviation term is given by

$$\Pi(t) = \frac{4}{3}\pi^{3/2} N_A C^{1/2} t^{1/2} \left(\frac{1 + 10.87x + 15.50x^2}{1 + 8.473x} \right). \tag{9}$$

In (9), N_A is the concentration of the acceptor ions (doping concentration N_0 in our case), C is the interaction parameter and

$$x = DC^{-1/3} t^{2/3} \tag{10}$$

is the normalized time variable with D being the diffusion coefficient. Values for coefficients C and D were calculated for each sample by applying a nonlinear least-squares fit to the decay curve of the $^3H_4$ level with equation (8), where $\Pi(t)$ is given by equation (9) and calculated average radiative lifetime were used. The measured decay curve of the $^3H_4$ level and the calculated best fit curve for the 5% Tm:LuAG sample are both shown in figure 6. The least-squares fit yielded $C = 6.74 \times 10^{-40}$ cm^6 s^{-1} and $D = 6.05 \times 10^{-12}$ cm^2 s^{-1} for the 0.5% Tm:LuAG, and $C = 1.70 \times 10^{-39}$ cm^6 s^{-1} and $D = 8.66 \times 10^{-12}$ cm^2 s^{-1} for the 5% Tm:LuAG sample. Using the calculated value for C and the average radiative lifetime τ_R for the $^3H_4$ level (see table 3), the critical distance parameter R_0, given by [6]

$$R_0 = (\tau_R C)^{-1/6}, \tag{11}$$

can be computed. R_0 is a measure of the strength of cross relaxation, and represents the distance among active ions for which cross relaxation rate equals the radiative decay rate [6]. In our study, R_0 values of 9.4 and 11.0 Å were obtained for the 0.5% and 5% Tm:LuAG samples, respectively, giving an average value of 10.2 ± 0.8 Å. This corresponds to a Tm^{3+} concentration of 9.42×10^{20} cm^{-3} or nearly 7 at.%. In other studies, average R_0 values of 17.9 and 7.3 Å were reported for thulium-doped $0.7TeO_2$:$0.3CdCl_2$ glass [6] and for thulium-doped $Ge_{30}Ga_2As_6S_{62}$ [22], respectively.

4. Conclusions

In conclusion, we have presented the results of spectroscopic measurements and analyses done on two Tm:LuAG crystals with Tm^{3+} ion concentrations of 0.5 and 5 at.%. Average values of 1041 ± 143 μs and 17.7 ± 3.4 ms were determined for the radiative lifetimes of the $^3H_4$ and $^3F_4$ levels based on the Judd–Ofelt theory. The fluorescence lifetime of the $^3H_4$ level

was measured to be 851 and 42.3 μs for the 0.5% and 5% TmLuAG samples, respectively, showing that the strength of cross relaxation increases with concentration. The fluorescence spectra further showed that the 1470 nm ($^3H_4 \rightarrow {}^3F_4$) emission vanished for the 5% sample, while its strength was 60% of the 1800 nm ($^3F_4 \rightarrow {}^3H_6$) emission for the 0.5% sample, also supporting the role of cross relaxation. In the same concentration range, the lifetime of the $^3F_4$ level decreased from 11.2 to 7.1 ms due to the enhancement of the nonradiative decay mechanisms. Using the fluorescence data and the results of the Judd Ofelt analysis, an average value of $1.2 \pm 0.2 \times 10^{-21}$ cm^2 was obtained for the emission cross section at 2023 nm. Finally, the average value of the critical distance parameter R_0 was determined to be 10.2 ± 0.8 Å by using the diffusion-limited relaxation model for cross relaxation.

Acknowledgments

We thank Umit Demirbas for his assistance in the experiments and Brian Walsh for providing the Tm:LuAG samples.

References

[1] Kmetec J D, Kubo T S and Kane T J 1994 Laser performance of diode-pumped thulium-doped $Y_3Al_5O_{12}$, $(Y, Lu)_3Al_5O_{12}$ and $Lu_3Al_5O_{12}$ crystals *Opt. Lett.* **19** 186

[2] Rodriguez W J, Naranjo F L, Barnes N P and Kokta M R 1994 Quasi-two-level laser operation of Tm:LuAG *Proc. Technical Digest of Conf. on Lasers and Electro-Optics* vol 8 p 174

[3] Barnes N P, Jani M G and Hutcheson R L 1995 Diode-pumped, room-temperature Tm:LuAG laser *Appl. Opt.* **34** 4290

[4] Scholle K, Heumann E and Huber G 2004 Single mode Tm and Tm,Ho:LuAG lasers for LIDAR applications *Laser Phys. Lett.* **1** 285

[5] Filer E D, Barnes N P and Morrison C A 1991 Theoretical temperature-dependent branching ratios and laser thresholds of the $^3F_4$ to $^3H_6$ levels of Tm^{3+} in ten garnets *Proc. OSA TOPS Advanced Solid-State Lasers* vol 10 p 189

[6] Sennaroglu A, Kurt A and Özen G 2004 Effect of cross relaxation on the 1470 and 1800 nm emissions in Tm^{3+}:TeO_2–$CdCl_2$ glass *J. Phys.: Condens. Matter* **16** 2471

[7] Judd B R 1962 Optical absorption intensities of rare-earth ions *Phys. Rev.* **127** 750

[8] Ofelt G S 1962 Intensities of crystal spectra of rare-earth ions *J. Chem. Phys.* **37** 511

[9] Vleck J H V 1936 The puzzle of rare-earth spectra in solids *J. Phys. Chem.* **41** 67

[10] Broer L J F, Gorter C J and Hoogschagen J 1945 On the intensities and the multipole character in the spectra of the rare earth ions *Physica* **11** 231

[11] Kaminskii A A 1990 *Laser Crystals* (Berlin: Springer)

[12] Carnall W T, Fields P R and Rajnak K 1968 Spectral intensities of the trivalent lanthanides and actinides in solution II. Pm^{3+}, Sm^{3+}, Eu^{3+}, Gd^{3+}, Tb^{3+}, Dy^{3+}, and Ho^{3+} *J. Chem. Phys.* **49** 4412

[13] Mehta P C and Tandon S P 1970 Spectral intensities of some Nd^{3+} β-diketonates *J. Chem. Phys.* **53** 414

[14] Kaminskii A A 1996 *Crystalline Lasers: Physical Processes and Operating Schemes* (Boca Raton, FL: CRC Press)

[15] Krupke W F 1971 Radiative transition probabilities within the $4f^3$ ground configuration of Nd:YAG *IEEE J. Quantum Electron.* **7** 153

[16] Sennaroglu A, Kabalci I, Kurt A, Demirbas U and Ozen G 2006 Spectroscopic properties of Tm^{3+}:TeO_2–PbF_2 glasses *J. Lumin.* **116** 79

[17] Kalaycioglu H, Sennaroglu A and Kurt A 2005 Influence of doping concentration on the power performance of diode-pumped continuous-wave Tm^{3+}:$YAlO_3$ lasers *IEEE J. Sel. Top. Quantum Electron.* **11** 667

[18] Moulton P F 1986 Spectroscopic and laser characteristics of Ti:Al_2O_3 *J. Opt. Soc. Am.* B **3** 125

[19] Sudesh V and Goldys E M 2000 Spectroscopic properties of thulium-doped crystalline materials including a novel host, $La_2Be_2O_5$: a comparative study *J. Opt. Soc. Am.* B **17** 1068

[20] Weber M J 1971 Luminescence decay by energy migration and transfer: observation of diffusion-limited relaxation *Phys. Rev.* B **4** 2932

[21] Yokota M and Tanimoto O 1967 Effects of diffusion on energy transfer by resonance *J. Phys. Soc. Japan* **22** 779

[22] Han Y S, Heo J and Shin Y B 2003 Cross relaxation mechanism among Tm^{3+} ions in $Ge_{30}Ga_2As_6S_{62}$ glass *J. Non-Cryst. Solids* **316** 302